Electronic Supplementary Information (ESI)

Novel Silicoaluminophosphate Molecular Sieves with CHA/GME Intergrowth Structures: Synthesis, Structural Elucidation and Catalytic Application

Dehua Wang,[a] Beibei Gao,[b] Miao Yang,[c] Dong Fan,[c] Peng Tian[c,*] and Zhongmin Liu[c,*]

[a] School of Pharmaceutical and Chemical Engineering, Taizhou University, Taizhou 318000, China.

[b] Green Catalysis Center and College of Chemistry, Zhengzhou University, Zhengzhou 450001, China.

[c] National Engineering Research Center of Lower-Carbon Catalysis Technology, Dalian National Laboratory for Clean Energy, Dalian Institute of Chemical Physics, Chinese Academy of Sciences, Dalian 116023, P. R. China.

*Corresponding authors, E-mail: tianpeng@dicp.ac.cn, liuzm@dicp.ac.cn.

Table of Contents

1. Supplementary Tables

Table S1 Structural Characteristics of ABC-6 Family Zeolites.

2. Supplementary Figures

Fig. S1 Simulated powder XRD patterns of the CHA/GME intergrowth zeolites. The stacking of the PerBU's in AABB- and AABBCC-sequences is disordered.

Fig. S2 TG and DTA curves of the as-synthesized (a) DNL-8 (sample 1) and (b) DNL-9 (sample 5) samples.

Fig. S3 FTIR spectra of the as-synthesized samples DNL-8 (sample 1) and DNL-9 (sample 5).

Fig. S4 (a) XRD patterns of the as-synthesized samples and (b) SEM image of sample 3.

Fig. S5 (a) XRD patterns and SEM images of (b) sample 6, (c) sample 7 and (d) sample 8.

Fig. S6 ^{27}Al and ^{31}P MAS NMR spectra of (a) sample 1 and (b) sample 3.

Fig. S7 (a) The length of *d6r* and (b,c) GME framework along the *c* and *a* axes, respectively.

Fig. S8 Methanol conversion and product selectivity in the methanol amination reaction on DNL-9 (sample 8) at 320 °C with a NH_3/CH_3OH molar ratio of 2/1 and methanol WHSV= 0.813 h^{-1}.

Fig. S9 NH_3-TPD profiles of DNL-9 (sample 8) and SAPO-34(B).

1. Supplementary Tables

Table S1 Structural Characteristics of ABC-6 Family Zeolites

Type materials	Code	Group Space	Sizes Ring	Stacking (Repeated layer) sequence	Building units
Cancrinite	CAN	$P6_3/mmc$	12 6 4	AB(A)....(2)	Single 6-rings only 12.25Å-12.70Å
Sodalite	SOD	*Im-3m*	6 4	ABC(A)...(3)	
Losod	LOS	$P6_3/mmc$	6 4	ABAC(A)...(4)	
Liottite	LIO	*P-6m2*	6 4	ABACAC(A)...(6)	
Afganite	AFG	$P6_3/mmc$	6 4	ABABACAC(A)...(8)	
Franzinite	FRA	*P-3m1*	6 4	ABCABACABC(A)...(11)	
Tounkite	TOL	*P-3m1*	6 4	CACACBCBCACB(C)...(12)	
Marinellite	MAR	$P6_3/mmc$	6 4	ABCBCBACBCBC(A)...(12)	
Farneseite	FAR	$P6_3/mmc$	6 4	ABCABABACBACAC(A)...(14)	
Giuseppettite	GIU	$P6_3/mmc$	6 4	ABABABACBABABABC(A)...(16)	
Offretite	OFF	*P-6m2*	12 8 6 4	AAB(A)...(3)	Double 6-rings and single 6-rings 12.85Å-13.20Å
ZnAlPO-57	AFV	*P-3m1*	8 6 4	AABCC(A)...(5)	
Erionite	ERI	$P6_3/mmc$	8 6 4	AABAAC(A)...(6)	
TMA-E(AB)	EAB	$P6_3/mmc$	8 6 4	AABCCB(A)...(6)	
ZnAlPO-59	AVL	*P-3m1*	8 6 4	ABBACCA(A)....(7)	
Levyne	LEV	*R-3m*	8 6 4	AABCCABBC(A)...(9)	
STA-2	SAT	*R-3m*	8 6 4	AABABBCBCCAC(A)...(12)	
Gmelinite	GME	$P6_3/mmc$	12 8 6 4	AABB(A)...(4)	Double 6-rings only 13.65Å-13.75Å
Chabazite	CHA	*R-3m*	8 6 4	AABBCC(A)...(6)	
SAPO-56	AFX	$P6_3/mmc$	8 6 4	AABBCCBB(A)...(8)	
AlPO-52	AFT	$P6_3/mmc$	8 6 4	AABBCCBBAACC(A)...(12)	
SSZ-52	SFW	*R-3m*	8 6 4	AABBAABBCCBBCCAACC(A)...(18)	

2. Supplementary Figures

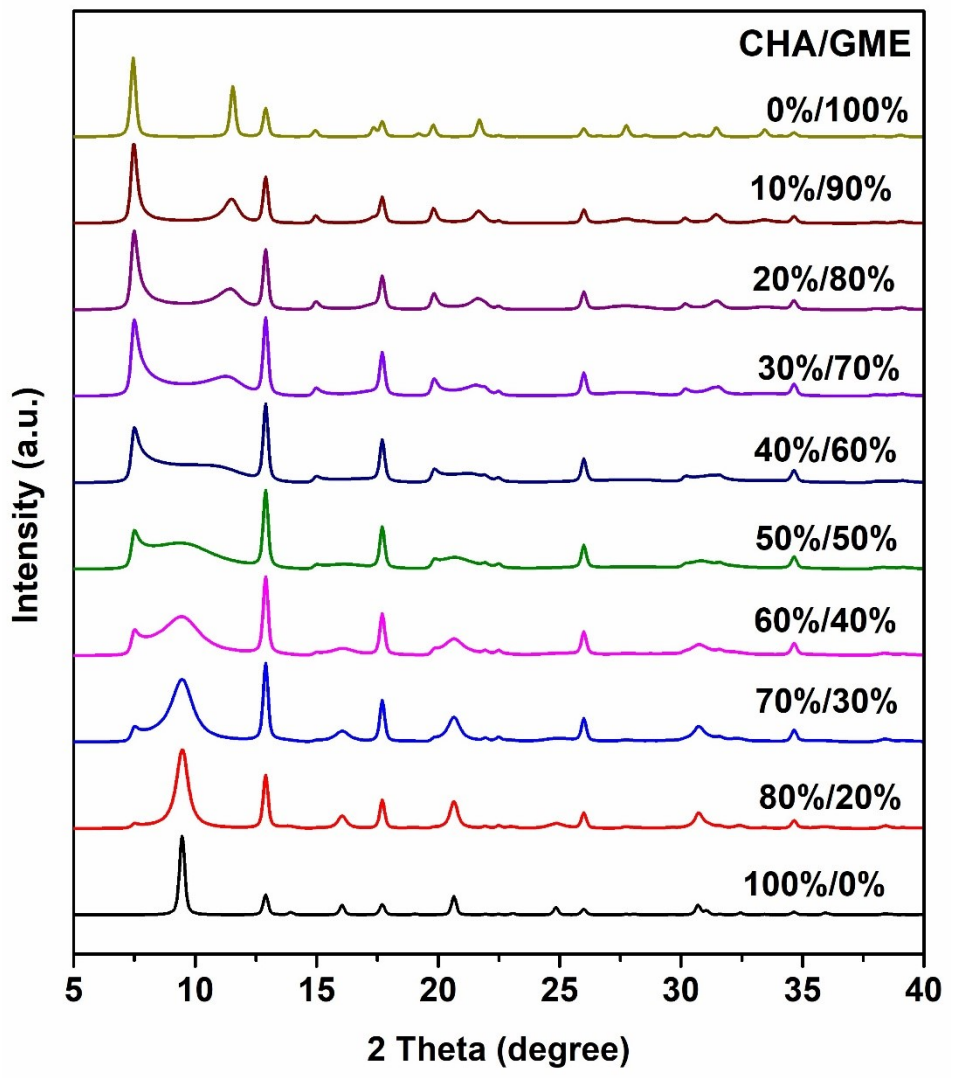

Fig. S1 Simulated powder XRD patterns of the CHA/GME intergrowth zeolites. The stacking of the PerBU's in AABB- and AABBCC-sequences is disordered.

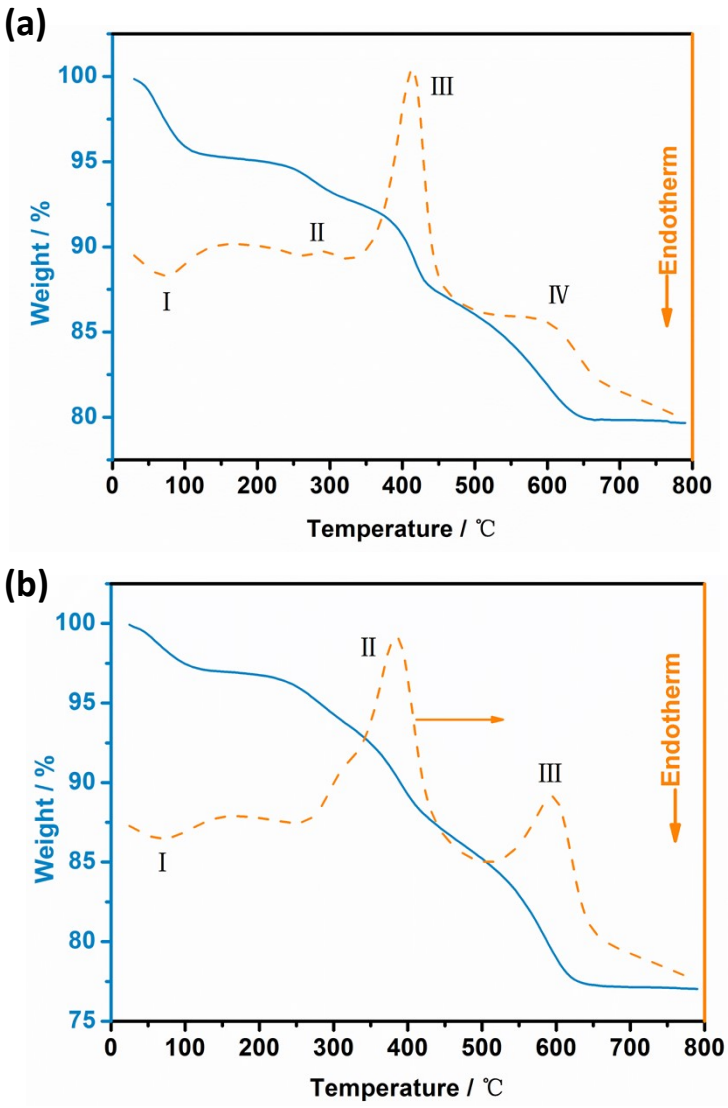

Fig. S2 TG and DTA curves of the as-synthesized (a) DNL-8 (sample 1) and (b) DNL-9 (sample 5) samples.

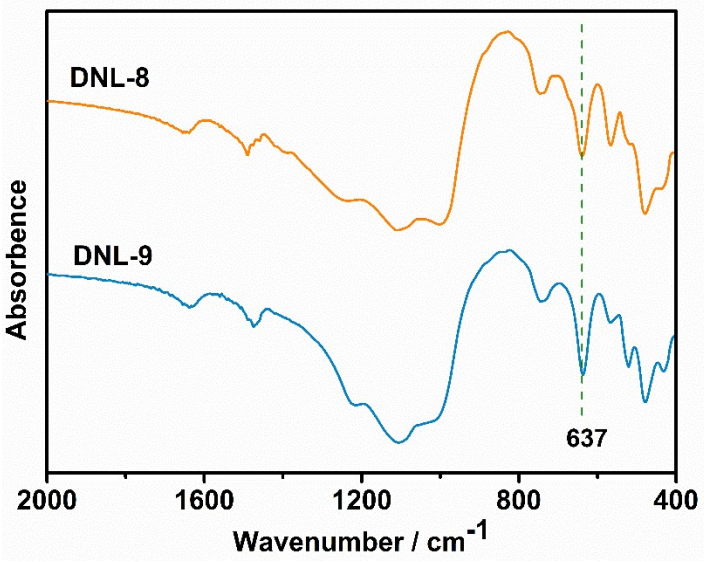

Fig. S3 FTIR spectra of the as-synthesized samples DNL-8 (sample 1) and DNL-9 (sample 5).

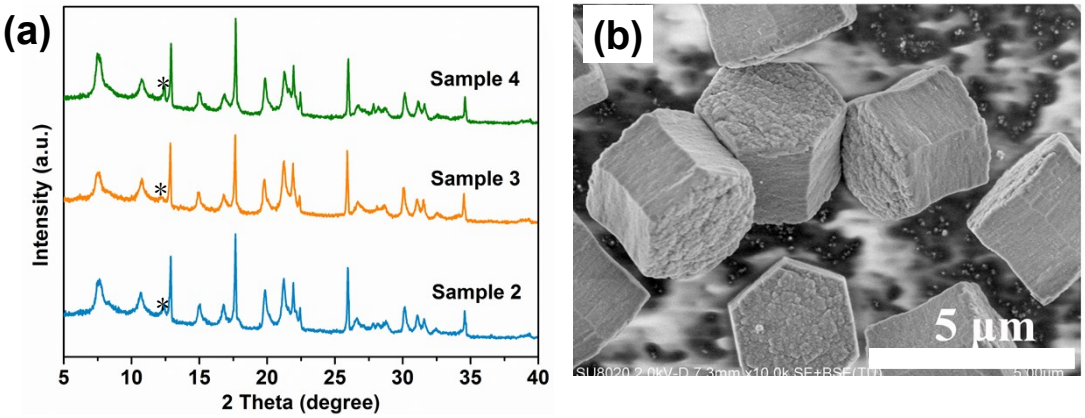

Fig. S4 (a) XRD patterns of the as-synthesized samples and (b) SEM image of sample 3.

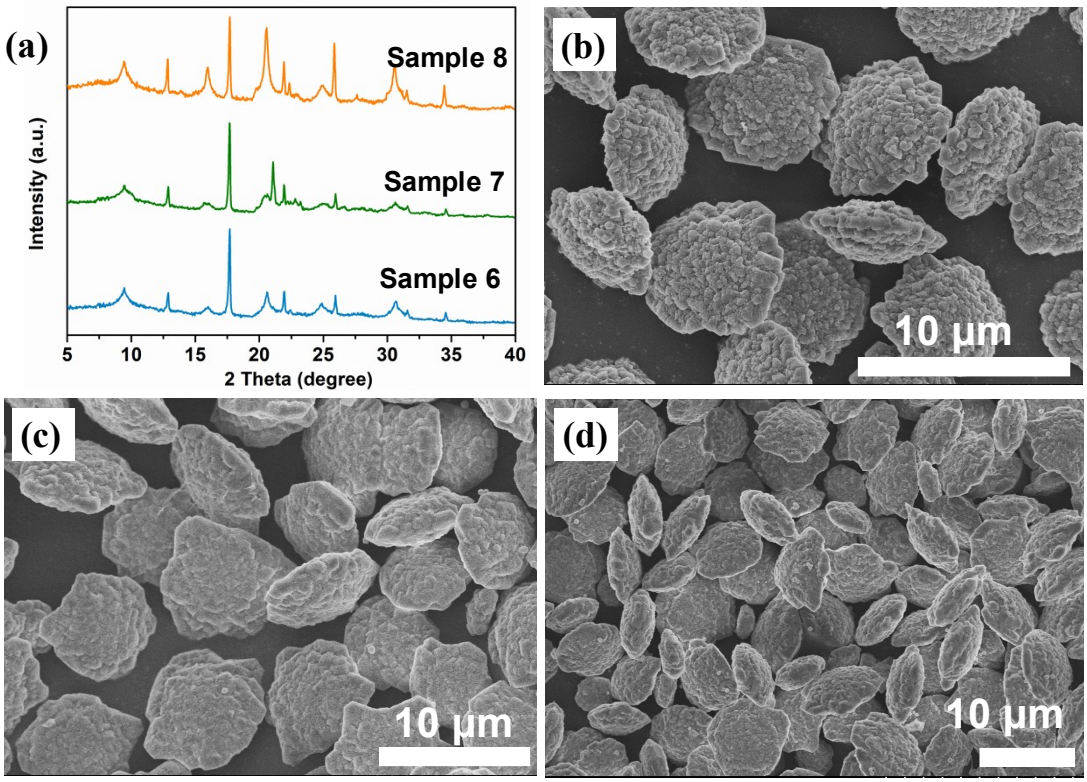

Fig. S5 (a) XRD patterns and SEM images of (b) sample 6, (c) sample 7 and (d) sample 8.

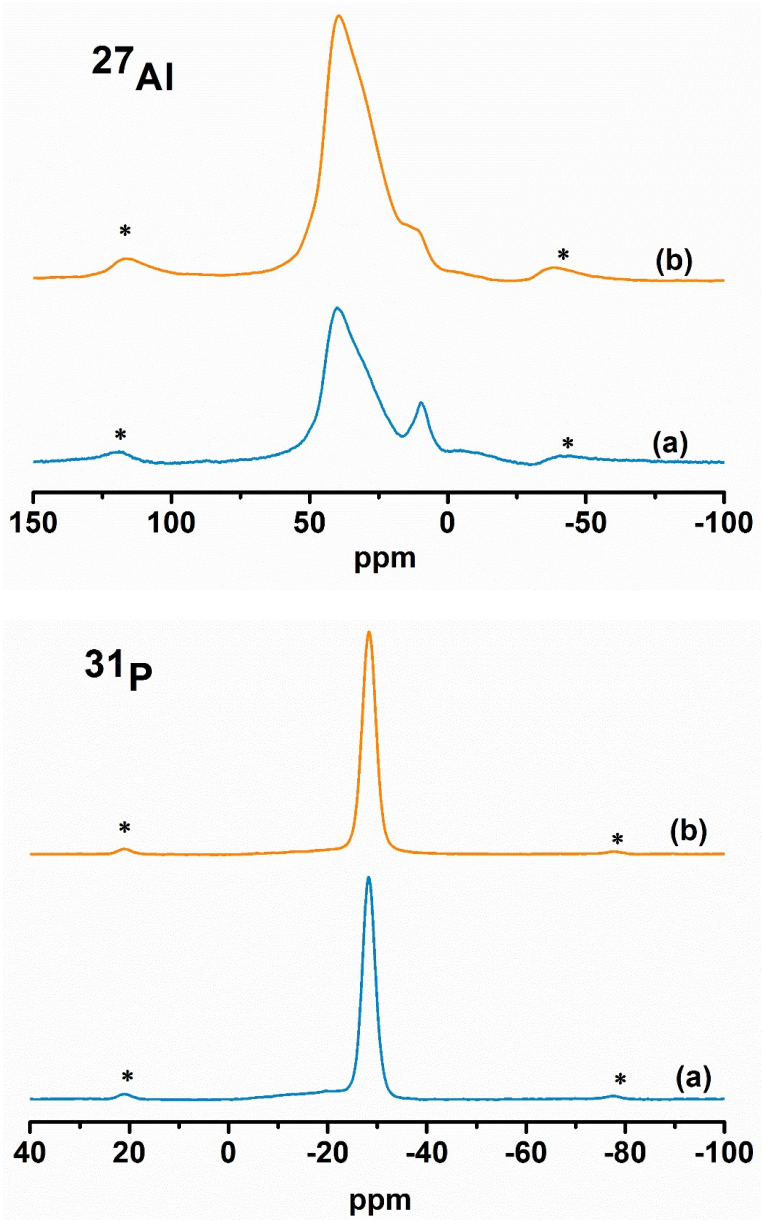

Fig. S6 ^{27}Al and ^{31}P MAS NMR spectra of (a) sample 1 and (b) sample 3.

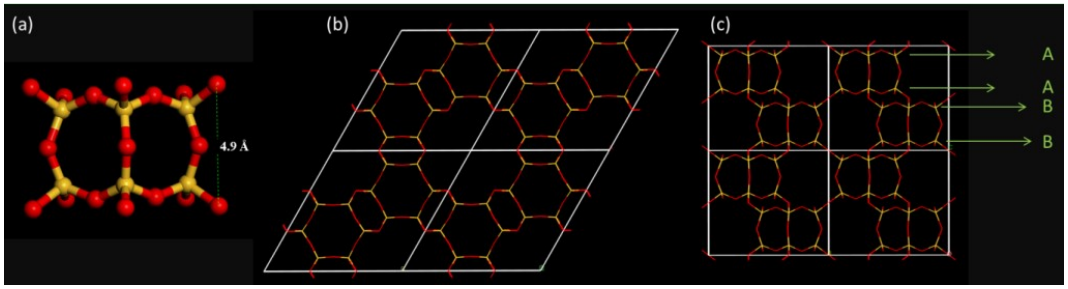

Fig. S7 (a) The length of *d6r* and (b,c) GME framework along the *c* and *a* axes, respectively.

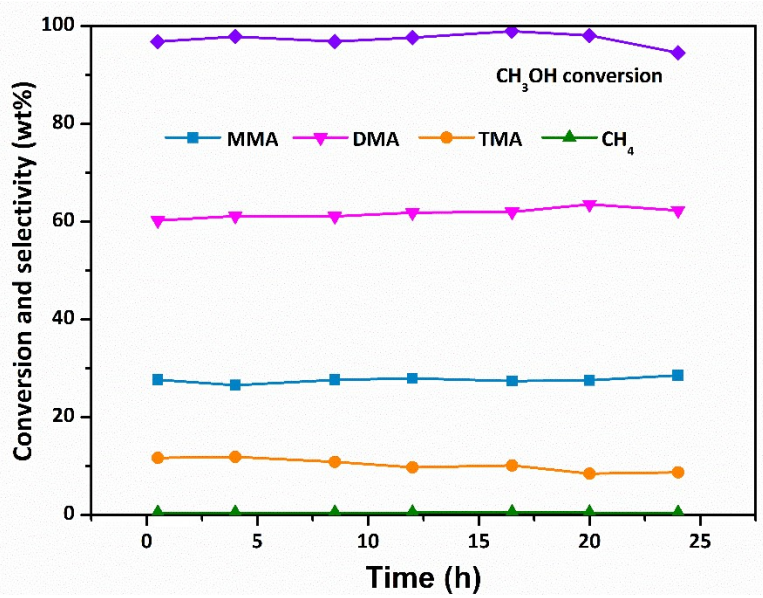

Fig. S8 Methanol conversion and product selectivity in the methanol amination reaction on DNL-9 (sample 8) at 320 °C with a NH_3/CH_3OH molar ratio of 2/1 and methanol WHSV= 0.813 h^{-1}.

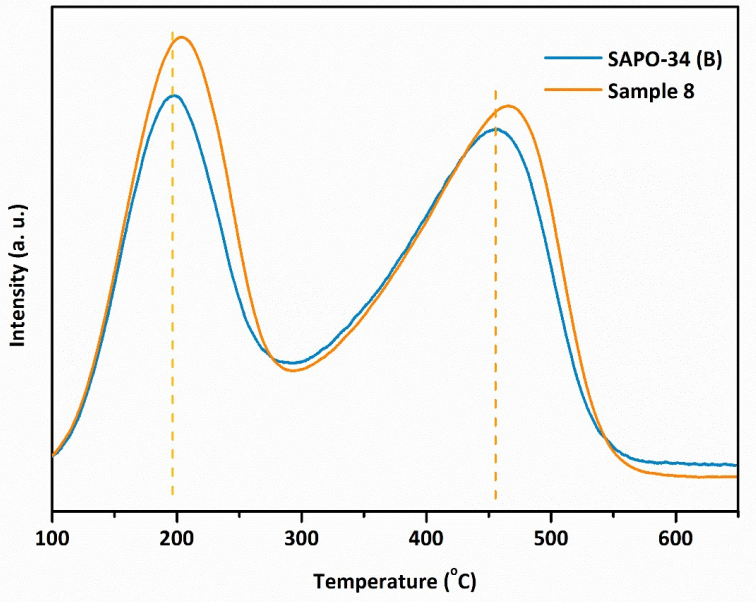

Fig. S9 NH_3-TPD profiles of DNL-9 (sample 8) and SAPO-34(B).

Note: Elemental compositions of DNL-9 (sample 8) and SAPO-34(B): $Al_{0.463}P_{0.330}Si_{0.207}$ and $Si_{0.216}Al_{0.461}P_{0.323}$, respectively. The gel molar composition for the synthesis of SAPO-34(B) is $0.9SiO_2 : 0.8P_2O_5 : 1Al_2O_3 : 50H_2O$: 2diethylamine (DEA), and the crystallization was carried out at 200 °C for 24 h.